Hindawi Publishing Corporation
Shock and Vibration
Volume 2016, Article ID 8794560, 17 pages
http://dx.doi.org/10.1155/2016/8794560

*Research Article*

# Experimental Investigation of Wave-Induced Hydroelastic Vibrations of Trimaran in Oblique Irregular Waves

**Haoyun Tang, Huilong Ren, Hui Li, and Qi Zhong**

*College of Shipbuilding Engineering, Harbin Engineering University, Harbin 150001, China*

Correspondence should be addressed to Haoyun Tang; conanthy@126.com

Received 29 September 2016; Revised 8 November 2016; Accepted 10 November 2016

Academic Editor: Mickaël Lallart



The irregular wave condition, especially the oblique irregular wave condition, is the actual circumstances when trimaran is sailing in sea. In order to identify the characteristic of the wave-induced hydroelastic vibration in irregular waves, as well as investigate the change of vibration in different oblique irregular wave conditions, trimaran model tests were conducted to measure vibrations, wave impact, and motion under different azimuth and wave height. The vibration on main hull, side hull, and cross-desk is measured and analyzed separately to observe the influence of irregular wave in different structural parts. The longitudinal vibration, transverse vibration, and torsion are also included in the model tests measurement to investigate the relationship between these vibration deformation components and parameters of the irregular waves. The wave-induced hydroelastic vibrations and whipping effect is extracted and analyzed to find influence of whipping and springing on the total vibration. Based on the analysis, the dangerous positions and the critical waves condition is introduced to ensure that the subsequent structural strength assessment is more reliable.

## 1. Introduction

Trimaran, as a kind of high performance ship, receives more and more attention. The new type ship is composed of one main hull, two side hulls, and two cross-decks. On the one hand, the advantageous wave interference caused by side hull gives trimaran a smaller resistance and better stability; on the other hand, complex cross-deck structure makes the investigation on trimaran's vibration more difficult [1].

In fact, the distinctive transverse vibration and wave impact on cross-desk increase the complexity of research on trimaran's wave-induced hydroelastic vibration greatly. In order to observe the wave-induced vibration more exactly, experts take numerous model tests. Hampshire et al. designed and carried out the load experiment at QinetiQ Rosyth by a segmented model [2]. The model had five segments along the length of the main hull and two segments in each side hull. Two beams attached the side hull to the main hull. The segments of main hull and side hull were connected separately by a beam of varying stiffness. Then the data was applied to the design and structure analysis of trimaran. Kennell used a kind of back-spline structure in the segment model to measure the main hull vibration [3]. The model test with self-waterjet apparatus was implemented in David Taylor Model Basin to observe the influence of vibration under different speeds. In China, Wang et al. and Hu et al. also took a series of trimaran model tests to analyze vibration on longitudinal and transverse structure in regular and irregular waves [4, 5].

So far, most cross-structure of trimaran model is idealized into a beam, which ignores the influence of wave slamming and air cushion on the wet cross-desk [6]. And the wave impact of trimaran shell in different longitudinal locations is also rarely given attention. In fact, motion of trimaran is drastic when ship is sailing in oblique waves. It is highly possible for the phenomenon of slamming on cross-desk to happen. Wave impact often causes some high transient local pressure on the ship's bodies and subsequently the whipping forces to the entire hull structures [7, 8]. In addition, the irregular wave condition is more close to the real ship environment. The model test in irregular waves will give us a further understanding about the trimaran situation in actual sea condition. So a model with complete shell is designed and used to take a series of experiments in irregular waves. The sensors record the motion displacement, accretion, impact pressure, and vibration in different wave height and azimuth. They form forms a complete structural response documentation

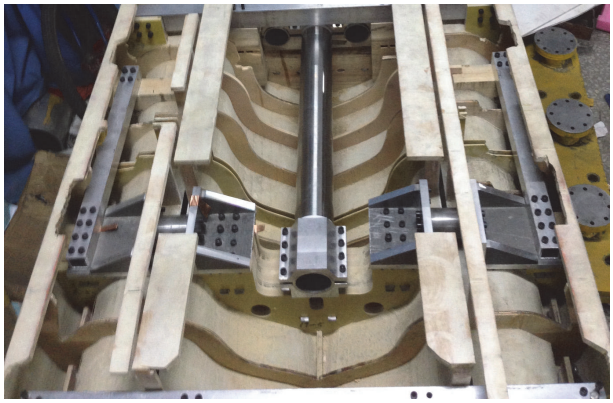

Figure 1: Trimaran backbone systems design.

of a trimaran, whose arrangement of side hull is at stern, in oblique irregular waves.

In this paper, the model design of trimaran and equipment is introduced. Then, these measured data are described and analyzed to study the characteristic of trimaran's kinds of motion and vibration response in the oblique waves. Meanwhile, the vertical vibration proportion of side hull in the whole trimaran is illustrated. And the difference of side hull vibration between wave forward surface and wave backward surface is observed and compared. The whipping and spring phenomenon is also extracted and analyzed by Fourier spectral analysis. And the distribution of pressure on trimaran shell, especially the gap of side hull between inside shell and outside shell, is also found and studied. Through this experiment and data analysis, there is a comprehensive understanding of the structural response of the trimaran under oblique waves. The conclusion made in paper will play a great role in guiding the structural design of trimaran and subsequent structural strength assessment.

## 2. Trimaran Model

*2.1. Hydroelastic Model Design.* The trimaran model consists of three longitudinal steel backbone systems and two transverse backbone systems. A series of variable cross-section circle ring beams were used to keep longitudinal stiffness of the main hull. The thickness of the rings was changed to meet the variation of stiffness on main hull. Two rectangle ring beams were installed to satisfy the stiffness on side hull. There were also two transverse beams to ensure the transverse stiffness of the trimaran. The pedestal was made of wood and combines with steel clamp to fasten these backbones. The vibration response was measured by the electric strain gauges mounted on these steel backbones. The specific design of backbone systems is shown in Figure 1.

The shell of model is made of fibre-reinforced plastic (FRP) with the scale ratio of 1 : 25 to ensure similar shell geometry. It is accurate to provide buoyancy and water hydrodynamic force. Meanwhile, the wave slamming and air cushion on the wet cross-desk are also considered by full simulation of trimaran's cross-desk. The trimaran shell is shown in Figure 2. In order to measure the distribution of

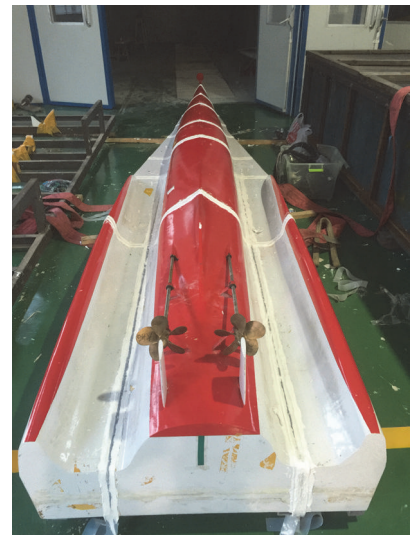

Figure 2: Trimaran model shell.

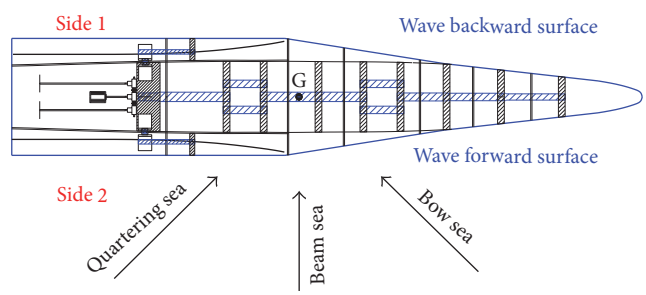


Figure 3: Final design of trimaran model.

Table 1: Division location of model.

| Division | Location from FP (m) | |
|---|---|---|
| | Model | Prototype |
| P1 | 1.02 | 25.4 |
| P2 | 1.56 | 39.0 |
| P3 | 2.04 | 50.9 |
| P4 | 2.72 | 67.9 |
| P5 | 3.19 | 79.8 |
| P6 | 4.28 | 107.0 |

longitudinal and transverse vibrations, the model is divided into seven segments along the length of the main hull and two segments in each side hull. The model is also divided into three segments to separate the main hull and side hull. The separating positions are given in Table 1. FP denotes fore perpendicular. The interval in each part of segments is 1 cm to satisfy the wave-induced hydroelastic vibration of the model [9, 10]. And the watertight in each interval was made by using the latex, which can be also observed in Figure 2.

In order to consider the influence of propeller on fluid and simulate the navigation of the trimaran, the propulsion system was installed in the last segment [11]. The self-propelled system is composed of an electric motor, driving devices, and two propellers. Finally, model design of trimaran is seen in Figure 3. The irregular waves came forward to the starboard

Figure 4: Four-degree-of-freedom monitoring instrument.

Table 2: Model dimensions.

| Description | Model | Prototype |
|---|---|---|
| Overall length (m) | 5.64 | 141 |
| Moulded breadth (m) | 1.06 | 26 |
| Depth (m) | 0.47 | 12 |
| Draft (m) | 0.2 | 5 |
| Displacement (t) | 0.255 | 3987 |
| VCG from BL (m) | 0.293 | 7.34 |
| LCG from FP (m) | 2.98 | 74.51 |
| Side hull length (m) | 2.44 | 61.00 |
| Side hull breath (m) | 0.15 | 3.75 |
| Side hull depth (m) | 0.33 | 8.25 |

of trimaran model with the wave azimuth that is 45 deg, 90 deg, and 135 deg, respectively. And the pressure gauges were installed on the ship shell at wave forward side. The dimensions of final model are shown in Table 2. In the table, VCG is vertical center of gravity, LCG denotes longitudinal center of gravity, and BL denotes baseline.

*2.2. Motion Measurement.* The four-degree-of-freedom monitoring instrument was used to measure trimaran model movements, which is shown in Figure 4. It recorded the motions of trimaran model in waves, as heave, pitch, and roll [12, 13].

Three acceleration sensors were installed to monitor the intensity of the model motion in waves. The first acceleration sensor was put at 0.494 m from fore perpendicular (FP) to observe the acceleration at bow. The second acceleration sensor was fixed at VCG for monitoring the acceleration on the whole model. And the location of the third acceleration sensor was 4.5 m from FP to get the acceleration condition at stern.

*2.3. Pressure Measurement.* In order to observe the phenomenon of slamming and study the water impact on the surface of the model more accurately, twenty pressure gauges

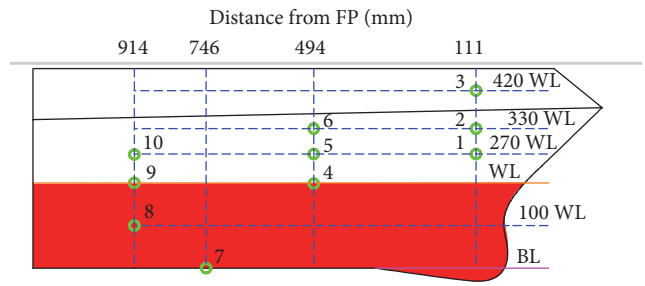


Figure 5: Pressure gauges arrangement at bow.

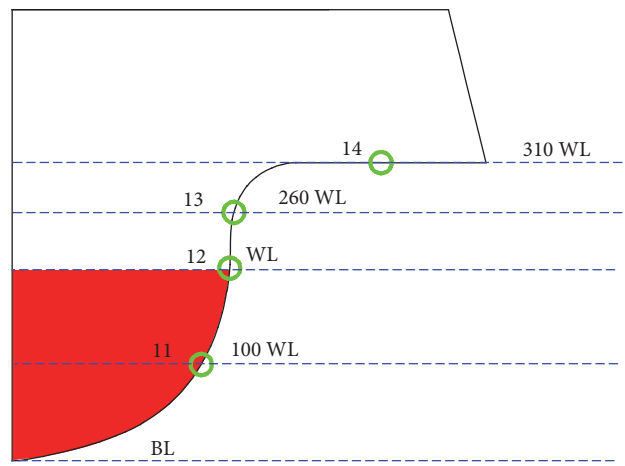


Figure 6: Pressure gauges arrangement amidships.

were installed at different locations along the length of the trimaran model [14, 15].

There are ten pressure gauges disposed at the first segment, as seen in Figure 5. And four pressure gauges were installed amidships. Figure 6 shows the specific location of these four pressure gauges. Then six pressure gauges were placed at 3.81 m from fore perpendicular (FP) to observe the water pressure at stern, as seen in Figure 7. The range of pressure gauges is from −100 Kpa to 100 Kpa. And then accuracy of these pressure gauges is 10 pa. The actual installation condition of these pressure gauges is shown at Figure 8.

*2.4. Simulation of Irregular Waves.* The experiment was carried out in ocean engineering tank of Harbin Engineering University. The length of tank is 50 m; the width is 30 m; and the depth is 10 m. The irregular waves were made by a hydraulically driven wave maker. The ISSC dual parameter spectrum is adopted in the irregular wave test [16, 17]. Wave time history curve is recorded by the wave height measuring instrument and shown in Figure 9.

The irregular wave data is converted into the waves of the real ship by use of the similitude rule. And the curve of wave spectrum density (WSD) is drawn out and compared with the theoretical wave spectrum. Figure 10 shows the comparison result in the W2 condition. The statistical significant wave height $H_S$ and the zero-crossing period $T_Z$ are calculated and

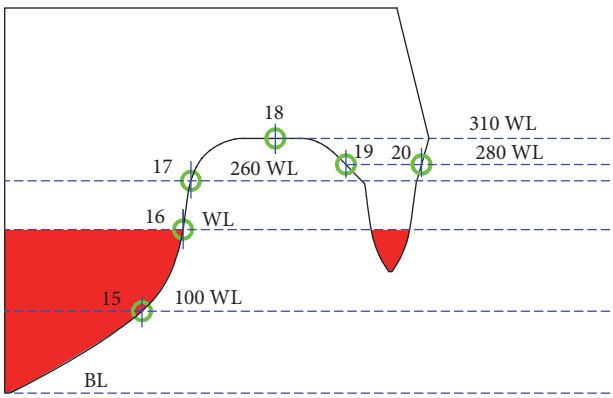


Figure 7: Pressure gauges arrangement at stern.

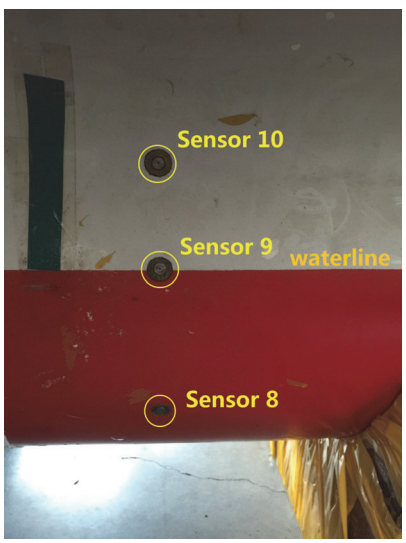


Figure 8: Pressure gauges arrangement.

Table 3: Comparison of irregular waves parameter.

| Scheme | Theory value | | Experiment value | | Deviation | |
|---|---|---|---|---|---|---|
| | $H_S$ (m) | $T_Z$ (s) | $H_S$ (m) | $T_Z$ (s) | $H_S$ | $T_Z$ |
| W1 | 4.2 | 6.70 | 4.18 | 6.63 | 0.51% | 1.04% |
| W2 | 4.0 | 6.70 | 3.98 | 6.59 | 0.42% | 1.64% |
| W3 | 3.8 | 6.70 | 3.79 | 6.73 | 0.18% | 0.45% |
| W4 | 3.6 | 6.70 | 3.58 | 6.67 | 0.48% | 0.45% |
| W5 | 3.4 | 6.70 | 3.38 | 6.71 | 0.71% | 0.15% |

compared with the theoretical ones. The deviation of irregular waves is illustrated in Table 3.

From the analyses of the irregular wave spectrum, it is found that the significant wave height measured is lower than the theoretical aim height. The deviation of the significant wave height is less than 1%. It can be explained that the irregular waves are attenuated when wave is propagating in tank. The zero-crossing period fluctuates around the theoretical target. And the error rate of the zero-crossing period is also less than 2%. Such results are considered as the influence

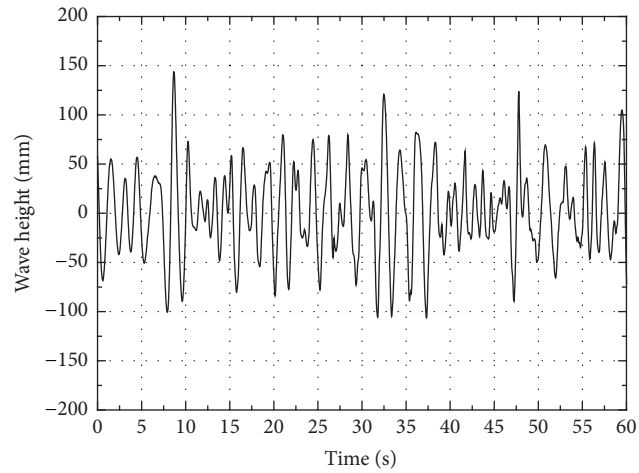


Figure 9: Irregular waves time histories.

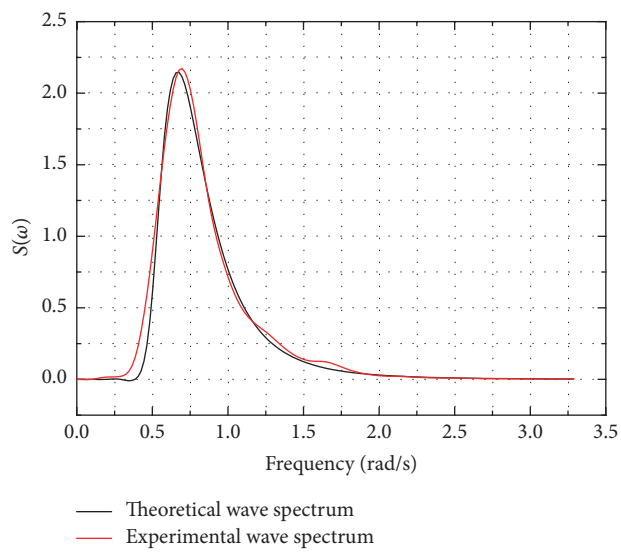


Figure 10: Comparison of wave spectral densities.

of the tank boundary. All these errors are in the acceptance range of this model experiment.

## 3. Experiment and Analysis

*3.1. Motion of Trimaran under Irregular Waves.* When ship is traveling in irregular waves, all the response on the ship is random, such as motion and vibration. So the statistical characteristic value is used as an indicator to express severity of motion and structural response. Autocorrelation function based spectral processing of the measured data was conducted to obtain the significant amplitude values. And all the analyses of motion and vibration are based on the corresponded statistical significant values. In addition, the amplitude of measured data is converted by the similitude rule before statistical analyses. The trimaran model ran with different azimuths and weights. These wave azimuth conditions include head sea, bow sea, beam sea, quartering sea, and

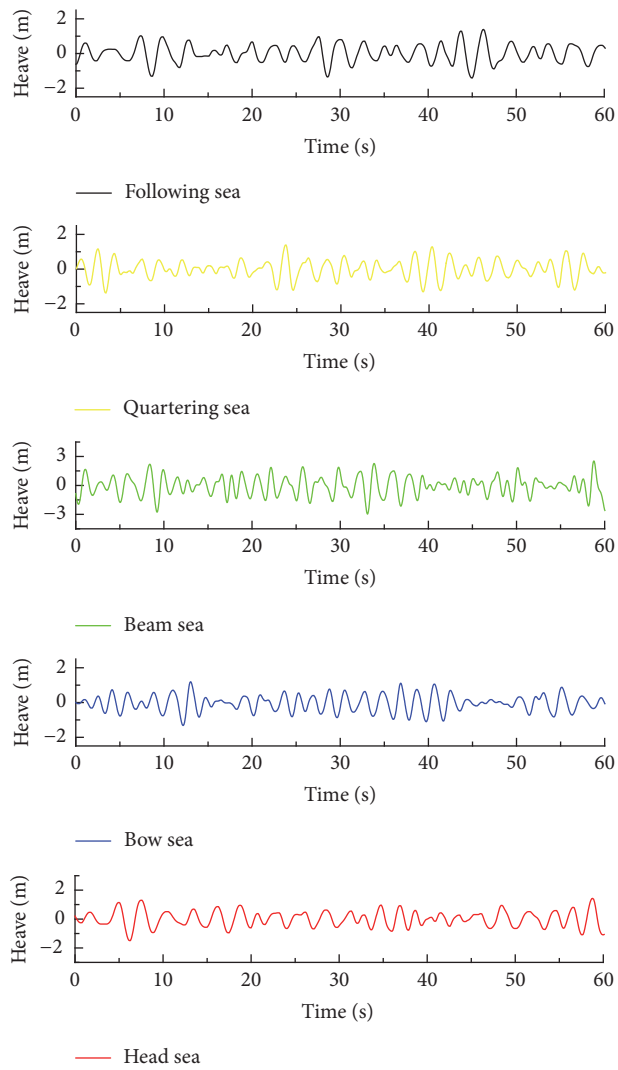


Figure 11: Time histories of heave in irregular waves.

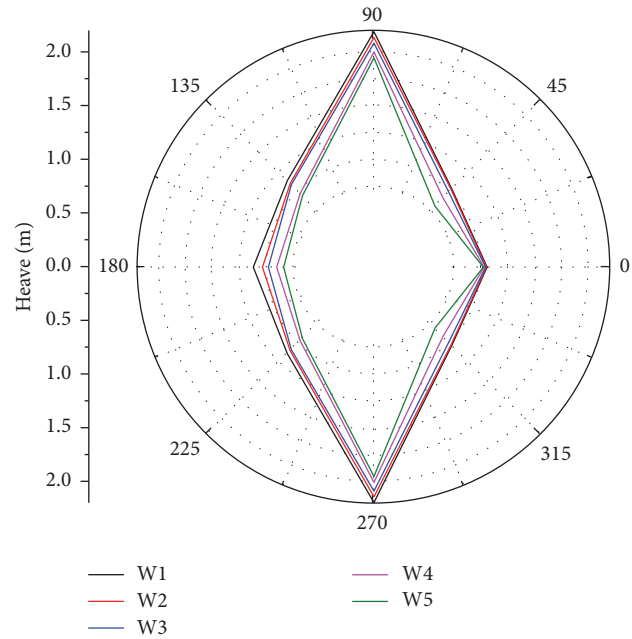


Figure 12: Results of heave in irregular waves.

following sea. And the wave weight conditions are from W1 to W5.

The heave motion is one of the important indicators on trimaran seakeeping performance. Its intensity affects the vertical vibration and the bottom water impact directly. Figure 11 shows the time history of trimaran heave in W2 oblique wave conditions. And the significant heave is calculated and shown in Figure 12. In polar diagrams of statistical results, the wave azimuth of heading wave condition is defined as 0 deg. And the wave azimuth in following wave condition is 180 deg. Similarly, the wave azimuth at 45 deg is representative of the bow sea condition. And the wave azimuth of quartering sea condition is 135 deg. Due to symmetry of the trimaran along the length of the hull, the response in the symmetric case is regarded as the same amount.

From Figure 12, it is found that the displacement of heave in beam sea is biggest among the irregular waves cases. The breadth is much less than the ship length, which makes lower resistance of wave-induced heave. So the heave in beam sea is more sensitive than other oblique waves conditions. Further, the displacement of heave in head sea is bigger than the ones in bow sea. The heave in following sea is gentler than this motion in quartering sea. It is also explained that the arrangement of side hull at stern reduces the intensity of heave displacement effectively. With the increase of wave height, the motion of heave is more severe compared to these wave cases from W1 to W5.

The pitch motion is one of the factors that cause the bow and stern slamming. And the serious slamming at bow is often the main cause of longitudinal whipping phenomenon. So it is necessary to find out the relationship between the displacement of pitch and different wave azimuths. Figure 13 shows the time history of trimaran pitch in W2 oblique wave cases. It can be observed that the pitch in beam sea is more frequent than the motion in other oblique wave cases. Then, the significant degree of pitch is collected and illustrated in Figure 14. Through comparative analyses, the response of pitch is more severe in head sea and following sea. Furthermore, the degree of pitch in following sea is higher than the value in head sea. The similar rule is found easily by comparing the quartering sea case with bow case. The arrangement of side hull increases the sensitivity of pitch when the wave comes from the trimaran's stern.

For a trimaran, roll is a kind of complex motion, when the interference of side hull is considered. Meanwhile, the severe roll will aggravate the extent of the impact on cross-deck, which may cause the transverse whipping phenomenon. So it is important to study the roll motion in oblique waves. Figure 15 shows the time history of trimaran roll in W2 oblique wave conditions. And the significant degree of roll is collected in Figure 16. The roll in beam sea is most severe among these wave cases. Further, the value of significant roll degree in beam sea is near to 1.5 times the value of significant

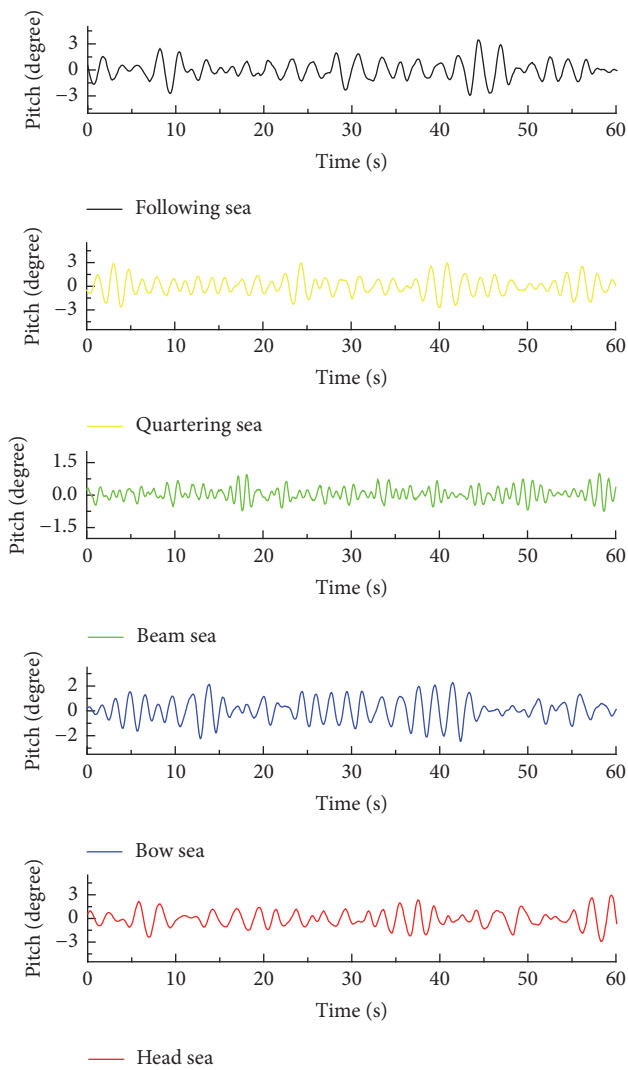


Figure 13: Time histories of pitch in irregular waves.

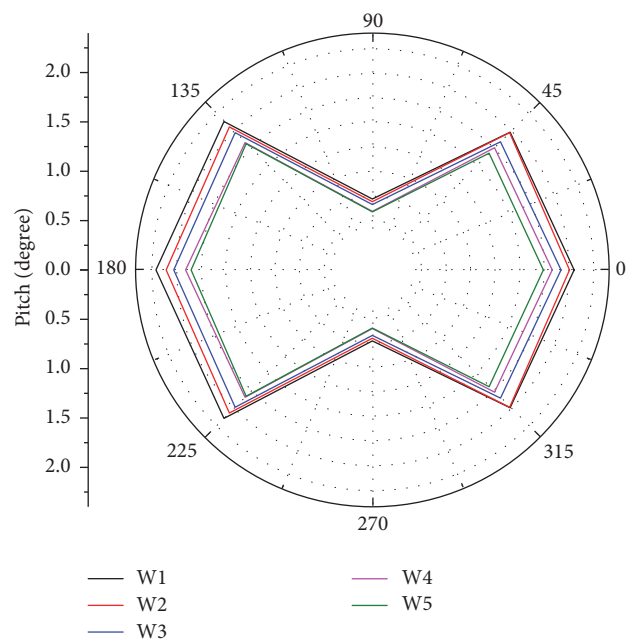


Figure 14: Results of pitch in irregular waves.

roll degree in other oblique waves. Obviously, the roll motion of trimaran would be aroused violently in beam sea. And the value of significant degree in bow sea is slightly higher than the one in quartering sea. The side hull arrangement at stern also can alleviate the severity of roll motion in quartering sea. In addition, it is known that the angle of pitch and roll is higher with the increasing of wave height.

The vertical acceleration in the motion is also recorded and analyzed. Figure 17 shows the time history of acceleration in beam sea. It can be observed that the time of acceleration peak appearance is very close at the three positions along the length of the ship. The acceleration at VCG is lower than the acceleration on the other places in Figure 18. The multiple influences of pitch motion and wave slamming widen the gap between the partial structure acceleration (bow and stern) and the whole ship acceleration. The bow acceleration is biggest in quartering sea and beam sea, which is replaced by stern acceleration in bow sea. The vertical acceleration raises smoothly with the increase of wave height.

*3.2. Load of Trimaran under Irregular Waves.* Dynamic wave load, which is the reflection of vibration response, is monitored by the steel backbone systems under irregular waves. The longitudinal steel backbone system on main hull recorded three kinds of vibration deformation on the main hull, such as vertical bending moment (VBM), horizontal bending moment (HBM), and torque. Two longitudinal steel backbone systems on the side hull also monitored the vertical bending moment of the side hull. And the splitting moments (SM) and transverse torsional moments (TTM) were observed by the transverse backbone systems. The data was collected and converted into corresponding statistical significant values. Then the analyses of these wave loads are done, respectively, as follows.

*3.2.1. Analyses of the Longitudinal Load under Irregular Waves*

*(1) Vertical Bending Moment Analysis.* The reaction of vertical bending deformation is always the most acute among the wave-induced vibration deformation. So the vertical bending moment becomes one of the most important components of the structural vibration response. It is a critical indicator in ship structural strength assessment.

Firstly, the vertical bending moment on the main hull is observed and studied. Figure 19 shows the VBM time history of main hull along the ship length in W1 oblique wave condition. Obviously, the time of VBM peak appearance is very close at P1, P4, and P6. There are consistent fluctuations along the length of ship. In Fourier spectral analysis, the method of Fast Fourier Transform algorithm and periodogram are used to translate these data from time domain into frequency domain. The spectral density function (PSD) is calculated by square root of mean squared amplitude (MSA), which is in proportion to amplitude of power spectrum, to analyze

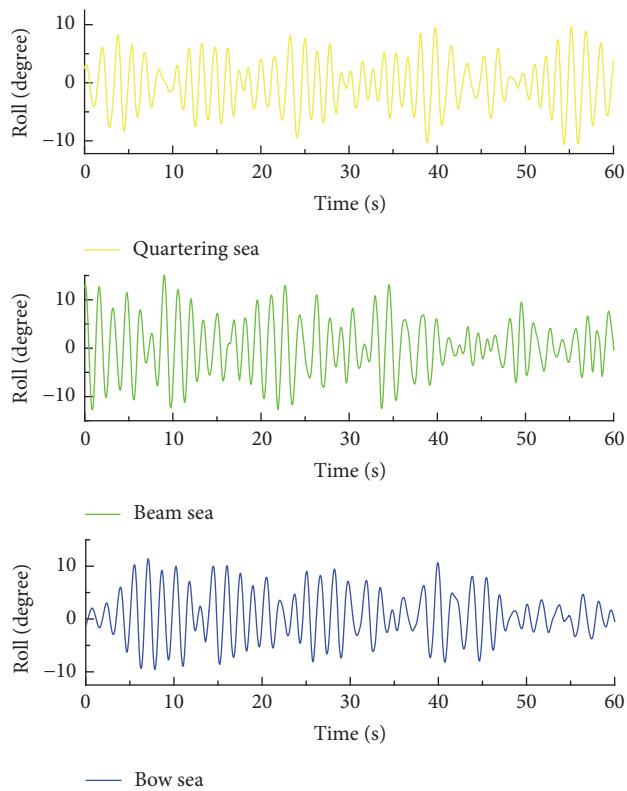


Figure 15: Time histories of roll in irregular waves.

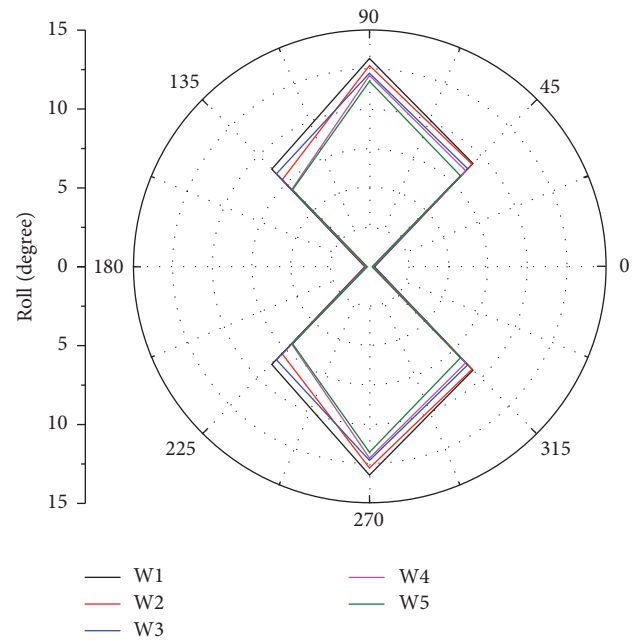


Figure 16: Results of roll in irregular wave.

characteristics of high frequency vibration. In Figure 20, the first peak frequency of VBM is ranged from 0.5 Hz to 1.08 Hz, which is the region of the encounter frequency of trimaran to the waves. The second high frequency vibration components caused by the hydroelastic vibrations focus around 5.12 Hz, which is close to the two-node natural frequency of vertical vibration (5.16 Hz). This high frequency vibration component does not fall from bow to amidships. In contrast, the high frequency vibration component at P4 occupies a larger proportion in PSD. The third high frequency vibration component appears obviously at P1 and P6. The range of this high frequency vibration is 10.41 Hz to 11.74 Hz and is not far from third-node natural frequency of vertical vibration (12.64 Hz). Similar phenomena are also observed in other oblique wave cases.

The reason of deviation between natural frequency and frequency peak of the hydroelastic vibration is analyzed. The low order natural frequency was measured by impact hammer test in calm water. In fact, when model was sailing in irregular waves, ship wetted surface was changed rapidly and all kinds of vibration responses by waves and experimental equipment were mutual interference. The surrounding flow field interference of model propeller and the vibration generated by propeller operation are considered as the reasons for the deviation between the natural frequency and measured high frequency peak. And some high frequency vibration caused by water slamming at both main hull and side hull's bow can also lead to this deviation.

Springing is a steady and periodic hull vibration by wave-induced forces. And this phenomenon occurs in the condition that the wave's encountered frequency or higher harmonic frequency matches with hull lower order natural frequency. Irregular waves contain a variety of waves with different frequencies, and it is relatively easy to stimulate this vibration. In Figure 21, the springing response of two-node natural frequency is found. The VBM amplitude of springing is extracted and compared with the significant VBM. The range of proportion on VBM caused by springing is from 7.34% to 10.19%. The position of maximum contribution of springing to significant VBM is amidships. And the vibration by springing at stern is bigger than the vibration at bow. Obviously, the arrangement of side hull intensifies this vibration at stern. The springing by three-node natural frequency is not obvious. And the higher order resonance is difficult to stimulate. The similar springing phenomenon is also found in bow sea and quartering sea condition, but the springing influence on hull significant VBM is weaker in comparison with its influence in beam sea.

The maximum location of VBM can be found in Figure 22 by counting the significant vertical bending moments at different positions. P4 is near amidships and suffers the severest vertical bending deformation. This location will not be changed in different wave height and azimuths. In addition, the VBM is higher with the increasing of wave height. Figure 23 shows the VBM of main hull in different azimuths. The significant VBM in beam sea is lowest among the oblique wave conditions. Because of the arrangement of side hull at stern, the trimaran suffers more severe vertical bending deformation in bow sea than the one in quartering sea. And the head sea is the most dangerous case for the vertical bending deformation. More attention should be given to

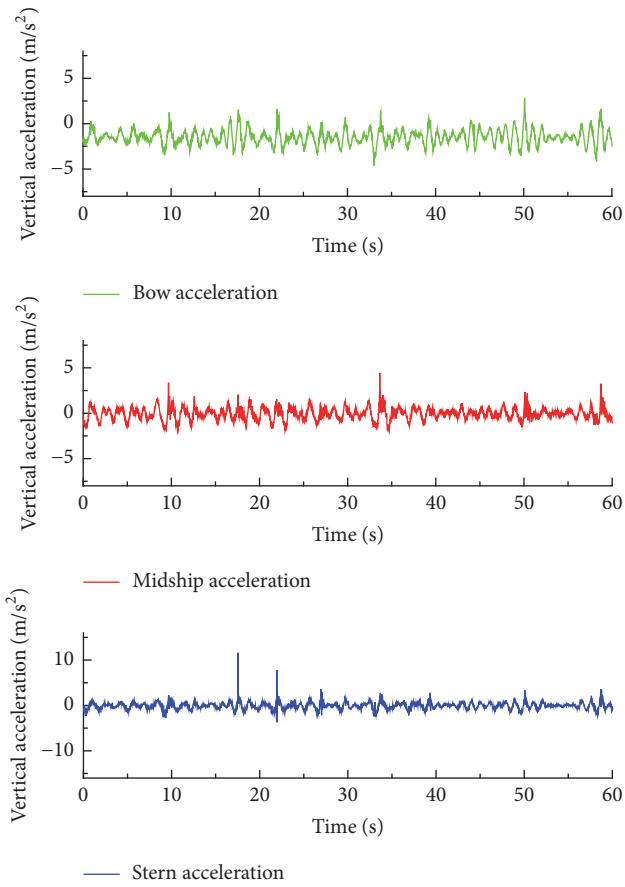


Figure 17: Time histories of acceleration in beam sea.

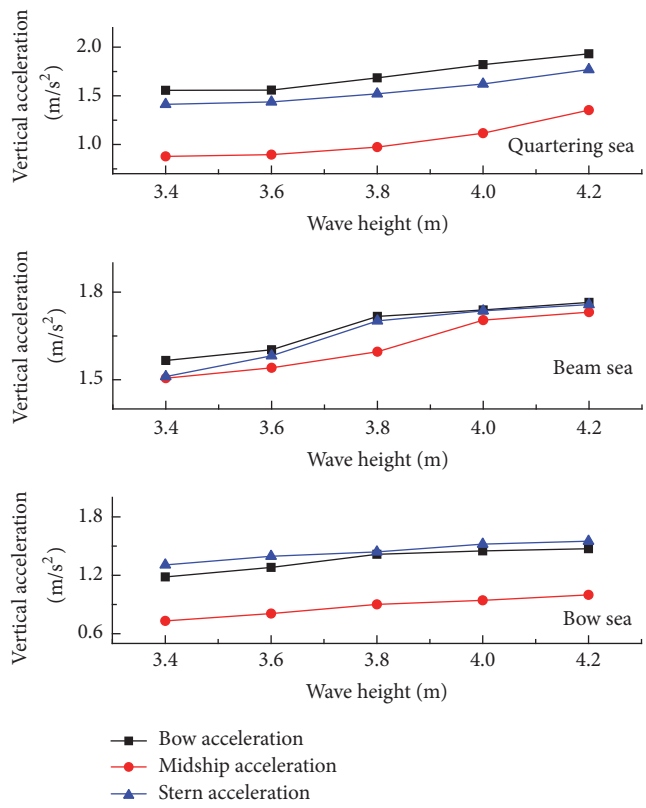


Figure 18: Results of acceleration in irregular waves.

the structure amidships in the structural vertical bending strength assessment.

Figure 24 shows the time history of the VBM at stern part of both side hull and main hull in W4 wave condition. Obviously the VBM fluctuations on the main hull and side hull remain consistent. The difference of side hulls is shown in Figure 25. Side 1 is at wave backward surface, and side 2 is wave forward surface. The VBM of side 2 is bigger than the values of side 1 in oblique waves. Further, the significant VBM ratio of side 2 to side 1 is ranged from 1.09 to 1.45.

The general significant vertical bending moment on the whole trimaran is often regarded as the sum of these three VBM components. So the significant vertical bending moment on the three structures is counted, and the ratios of VBM on each part to the general significant vertical bending moment are showed in Figure 26. From the ratios result of VBM, it can be seen that the ratio range of side hulls is from 8% to 32%, and this ratio gets the maximum proportion in beam sea. Meanwhile, the VBM difference between side 1 and side 2 reaches the peak. The max difference ratio is 9.77% and it also happens in beam sea, no matter that the general significant vertical bending moment is decreasing compared with other azimuths.

*(2) Horizontal Bending Moment Analysis.* When trimaran is sailing in oblique waves, it suffers a very complex structural

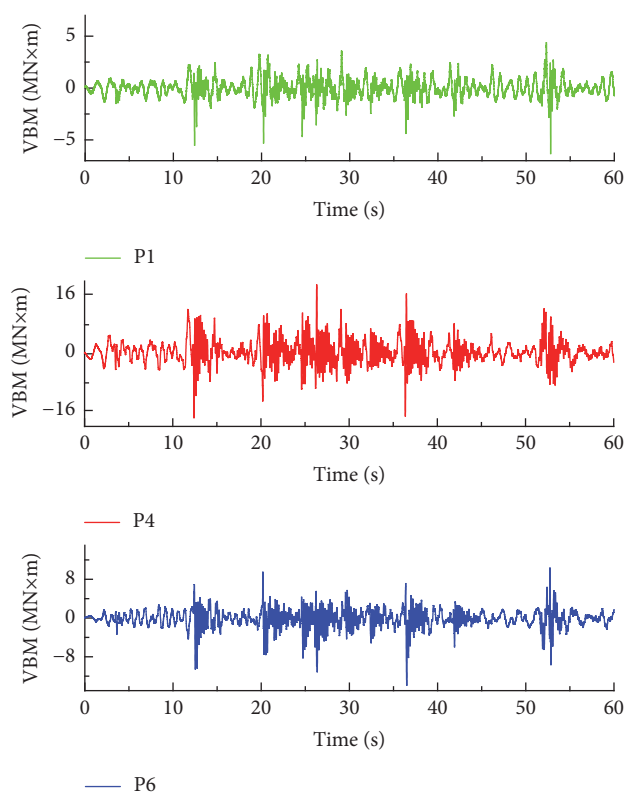


Figure 19: VBM time histories of main hull in beam sea.

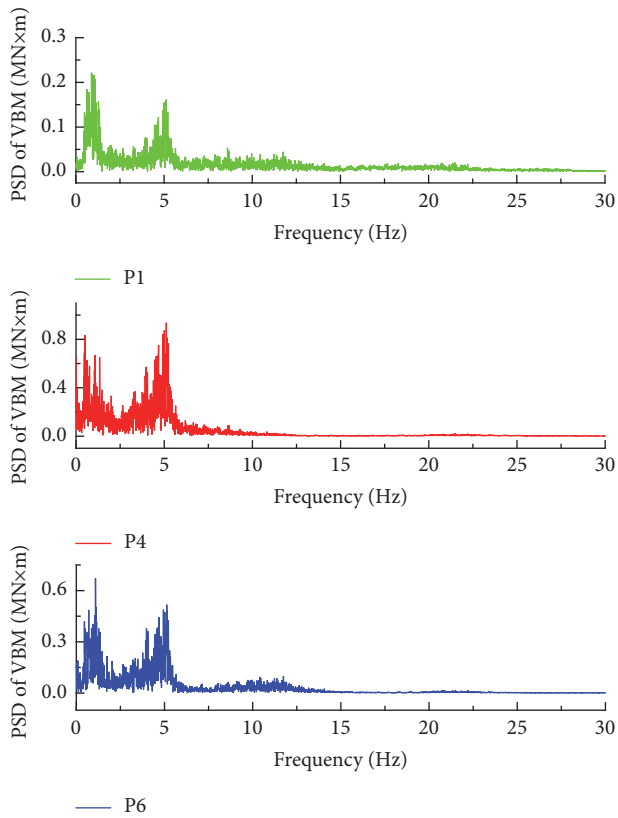


Figure 20: Power spectral density functions of VBM.

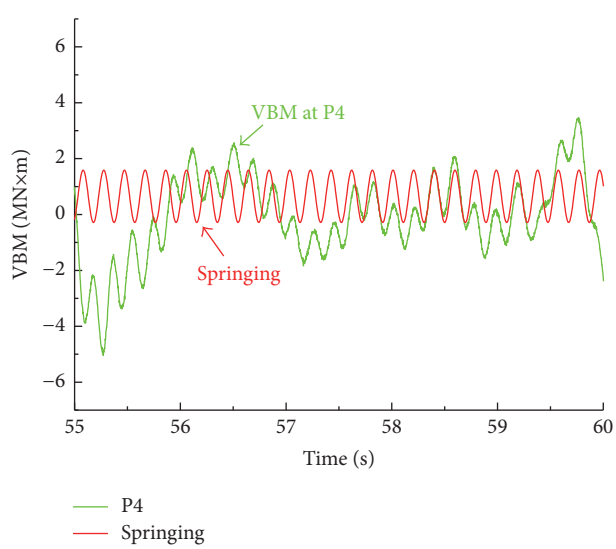


Figure 21: VBM time histories of springing.

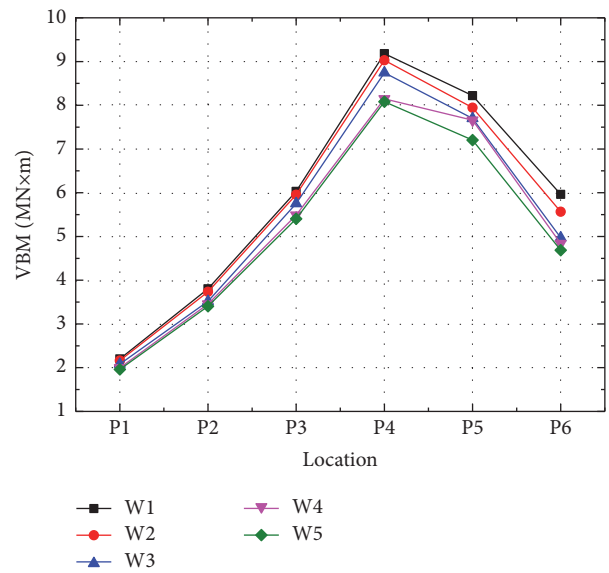


Figure 22: Longitudinal distribution of VBM in beam sea.

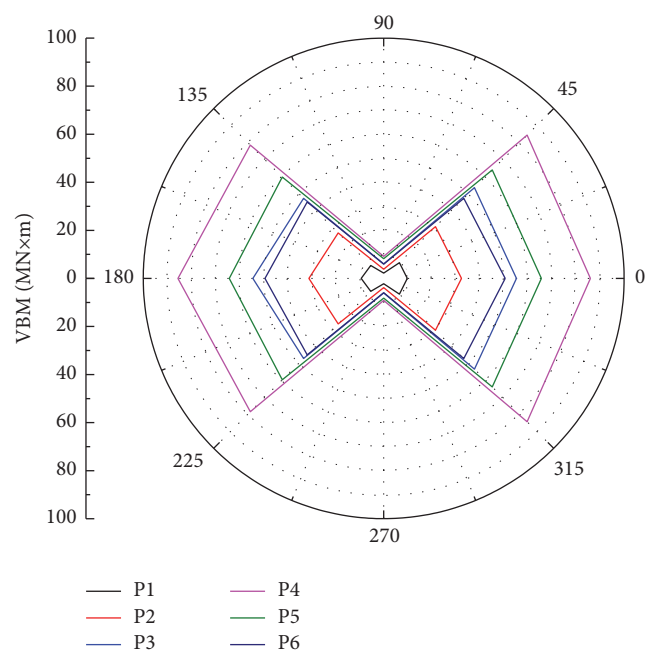


Figure 23: VBM of main hull in different azimuths.

response along the ship length, which is not only the vertical bending deformation but also the horizontal bending deformation and torsion. In oblique wave cases, the horizontal bending vibration and torsion often have strong reaction, even more violent than vertical bending deformation. The phenomenon is observed by Hu et al. [5] in trimaran model test, and it is also found in beam sea by comparing the data of horizontal bending vibration and vertical bending deformation. In beam sea cases, the value amidships of horizontal bending vibration is twice as much as the value of vertical bending vibration sometimes. It can be explained that the beam sea condition can arouse strong reaction on horizontal bending vibration, but it is hard to motivate the vertical bending vibration. When waves propagated in beam sea, the wave impacted on the side hull at stern first. This vibration was transmitted to main hull at stern by cross-deck structure. Then, waves reached the main hull and caused another vibration response of main hull. Superposition of these vibrations on horizontal direction formed trimaran's

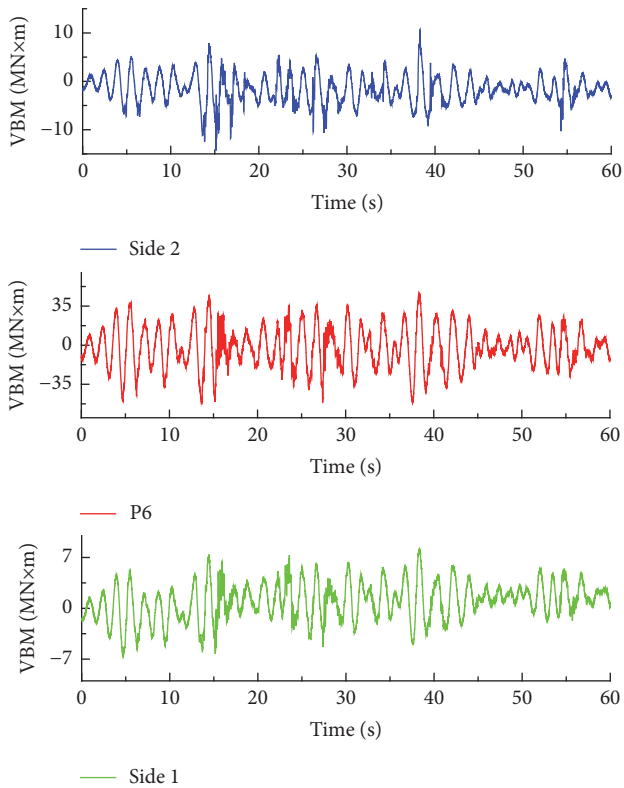


Figure 24: VBM time histories of main and side hull.

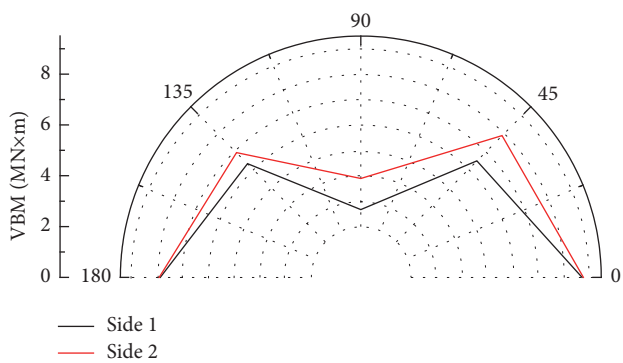


Figure 25: VBM of side hull in difference azimuths.

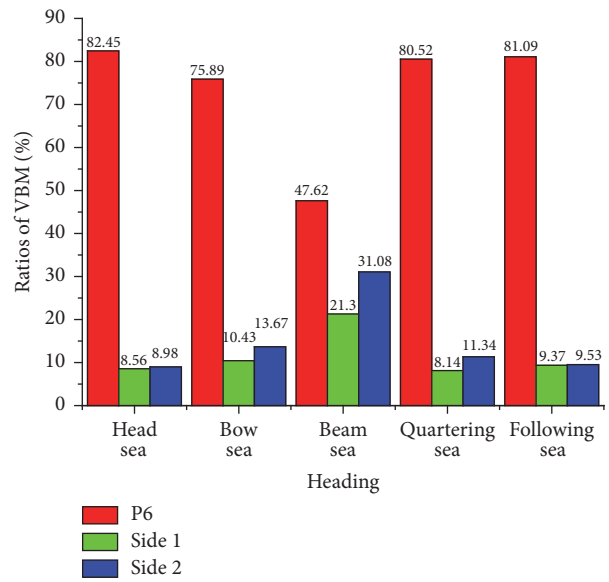


Figure 26: Ratios of VBM on main hull and side hull.

horizontal bending vibration. Obviously, the arrangement of side hull at stern further enhances the horizontal bending deformation, compared with ordinary monohull ship. Therefore, the horizontal bending vibration in oblique waves cannot be neglected. The horizontal bending moment, which represents the intensity of horizontal bending deformation, should be given more attention.

Figure 27 shows the HBM distribution along the length of ship. The significant HBM reach peak at P5 in beam sea, and two peaks (P3 and P5) are found in bow sea and quartering sea. In addition, P3 replaces P5 as the location suffered the horizontal bending vibration deformation most severely in quartering sea. Obviously, the significant HBM is increased with the development of wave height and adds greatly at P3, P4, and P5, whose location is amidships. The HBM distribution in different azimuths is introduced by Figure 28. It is almost impossible for the horizontal bending vibration deformation to happen in head sea and following sea. The HBM in beam sea is smallest in these oblique waves. And the horizontal bending vibration deformation in bow sea reflects most severely. It is explained that the arrangement of side hull at stern strengthens the stiffness of the whole ship structure and resists the horizontal bending vibration deformation at stern.

The power spectral density function of HBM is calculated by Fourier spectral analysis, as shown in Figure 29. The similar phenomenon like VBM is found in horizontal bending vibration deformation. The interval of HBM first peak frequency is from 0.225 Hz to 1.56 Hz. The high frequency horizontal vibrations are around 7.40 Hz. Further, the HBM at bow and stern get more high frequency horizontal vibrations. The springing also happened in horizontal bending vibration. The range of proportion on HBM caused by springing is from 5.01% to 7.29%. And the position of maximum contribution of springing to significant HBM is at bow.

*(3) Longitudinal Torque Analysis.* Although torsion deformation is hard to observe and measure, it is an indispensable load in oblique waves. It often makes important contributions to the damage of local structure and weakens the structural resistance. In order to measure the torsion on main hull, the variable cross-section circle ring beams are adopted and designed specifically. And the measured data of torsion deformation was collected and analyzed as indicated in Figure 30.

Figure 30 shows the torque distribution along the length of ship with different wave height. It is not hard to find that the torsional deformation is more serve with the increase of wave height. And the value of significant torque increases from bow to amidships. Then the significant torque falls at P5, where the side hull is arranged. Finally, the torsional deformation reaches the peak of torsional deformation at stern. The reason

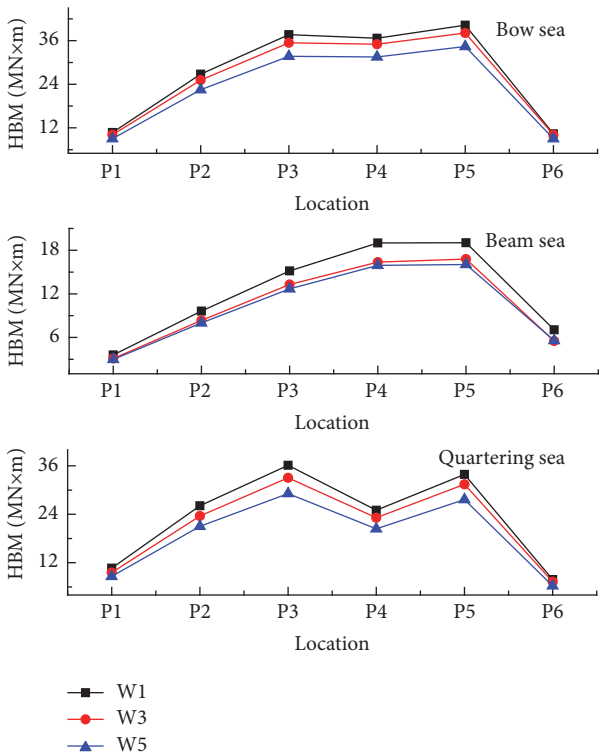


Figure 27: Longitudinal distribution of HBM.

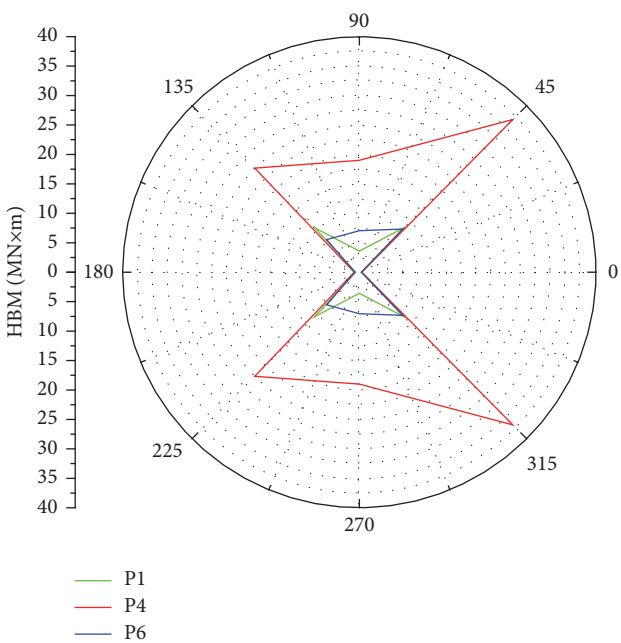


Figure 28: HBM of main hull in different azimuths.

of torque falling at P5 is explained where the sharp increase in torsional stiffness caused by side hull structure alleviates the torsional deformation, and the structure of side hull also takes more torsional load for trimaran, which increases the torque at stern again.

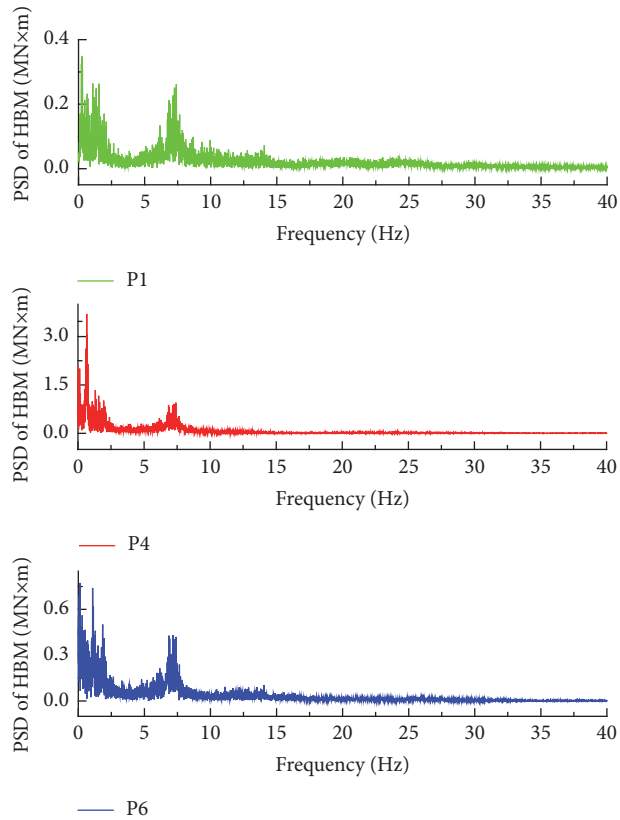


Figure 29: Power spectral density functions of HBM.

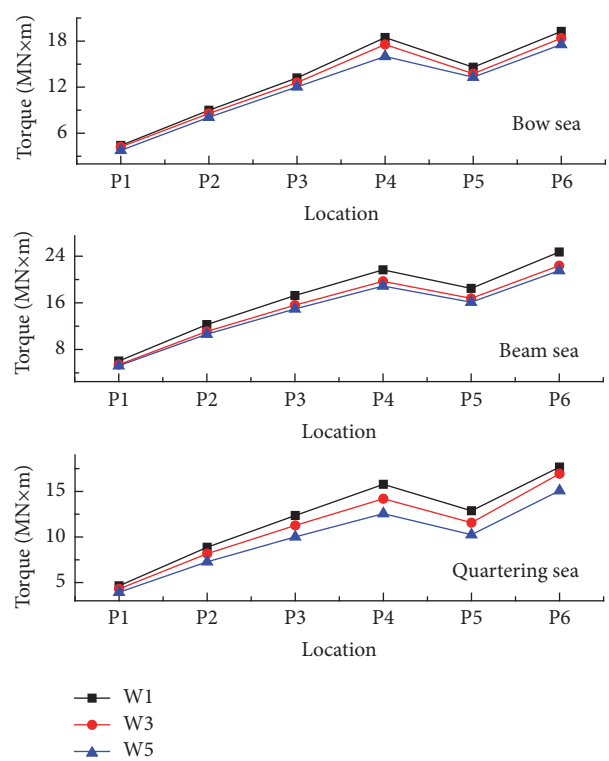


Figure 30: Longitudinal distribution of torque.

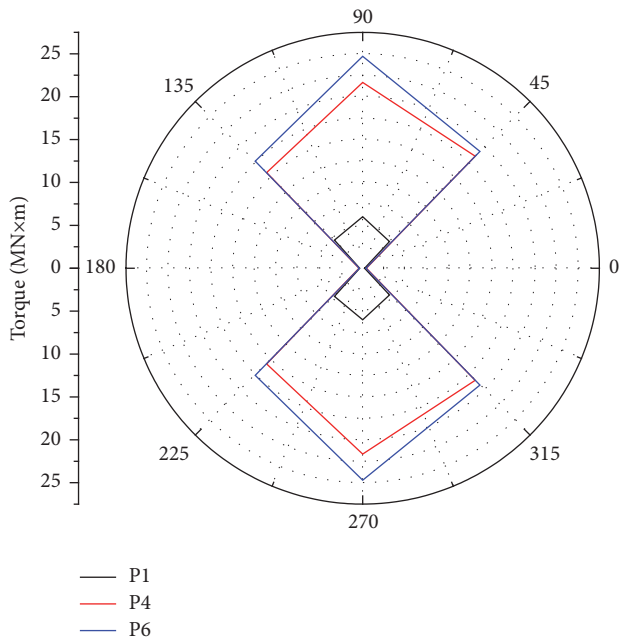


Figure 31: Torque of main hull in different azimuths.

The phenomenon that torsion deformation in beam sea is more serve than the deformation in other azimuths is observed in Figure 31. The torque value in beam sea is almost 1.2 s times as much as the value in bow sea and quartering sea. In addition, the similar phenomenon that torsion deformation is more violent than vertical bending deformation in beam sea also exists. There is a strong reaction of torsion deformation aroused in beam sea, but the reaction of vertical bending deformation in beam sea is smallest among the oblique waves conditions. The vibration influence of side hull at stern and the difference of load response between wave forward side and backward side aggravate torsion deformation. All these factors lead the torsion to be an important load in beam sea.

The Fourier spectral analysis is also made in torque time history. Only one frequency peak is found in the frequency domain. And the high frequency peak does not appear. Obviously, the torsion natural frequency is too high to be stimulated. From above analyses it is known that the stern of trimaran structure in beam sea is the critical cross-section for structure strength analyses.

*3.2.2. Analyses of the Transverse Load under Irregular Waves.* The observation on transverse deformation of trimaran is one of the aims of the model experiment. The individual transverse load for trimaran is splitting moment and transverse torsional moment, which is the potential cause of cross-deck structural break. The transverse backbone systems measure the potential danger and these data are analyzed as follows.

*(1) Splitting Moment Analysis.* The transverse bending deformation always exists when trimaran is sailing in oblique waves. It is a primary factor considered in the trimaran design of transverse structure.

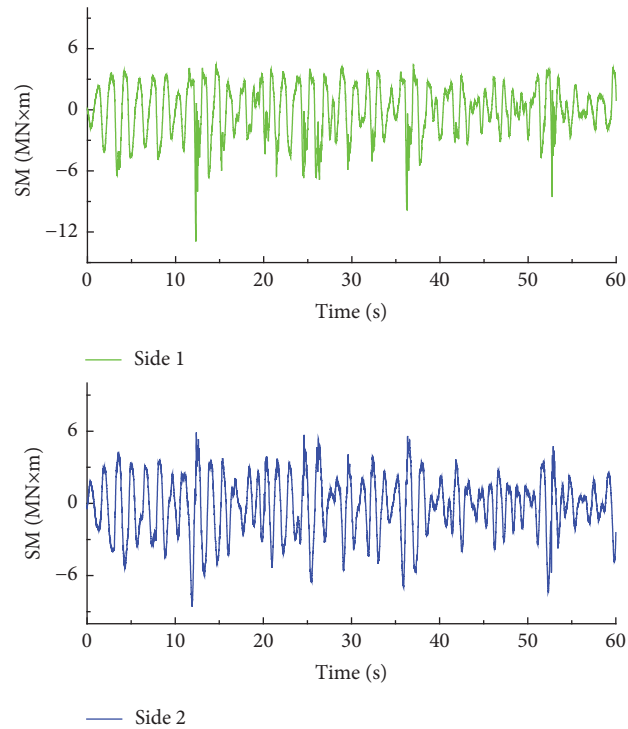


Figure 32: SM time histories in beam sea.

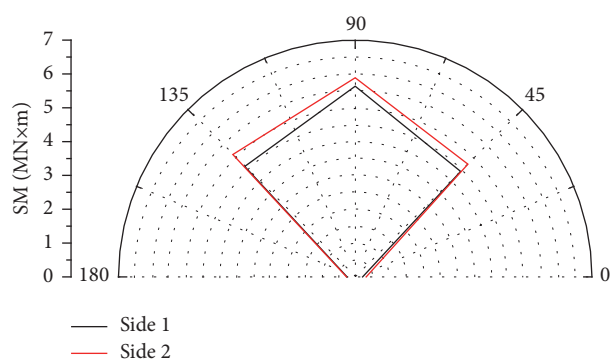


Figure 33: Splitting moment in different azimuths.

Figure 32 shows the splitting moment time history of the transverse cross-desk in beam sea. It can be observed that the peak of the splitting moment happens at the same time. Then, the time history data in different azimuths and wave heights were collected and processed. In Figure 33, it can be seen that the significant SM in beam sea is highest in oblique waves. And the trimaran suffers more severe SM in quartering sea than the ones in bow sea. The splitting moment at side 2 is always higher than the measured moment at side 1 and gets maximal gap in quartering sea. The principle in different wave height is analyzed in Figure 34. The SM in beam sea and bow sea increase rapidly with the rise of wave height. But the SM in quartering sea tends to be gentle in higher wave height. This rule fits both side 1 and side 2. The high frequency peak of SM also is not notable like torsion in the Fourier spectral analysis. Therefore, then effect

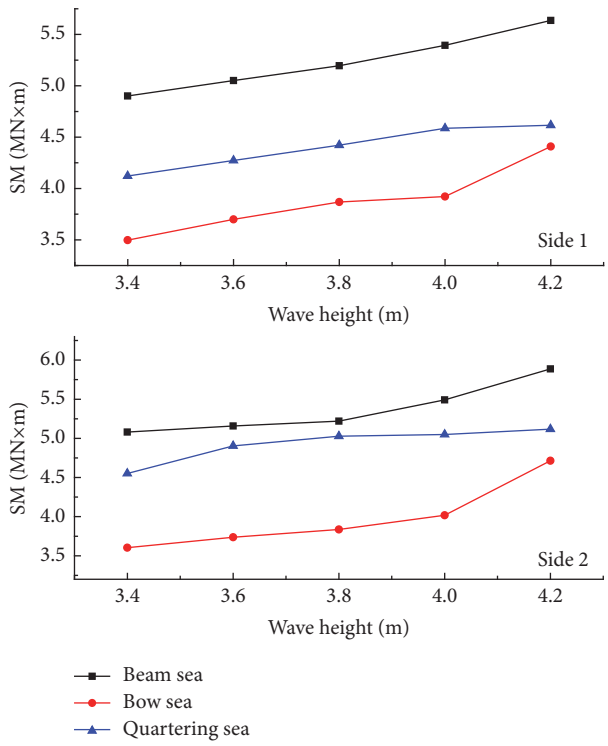


Figure 34: Splitting moment in different wave height.

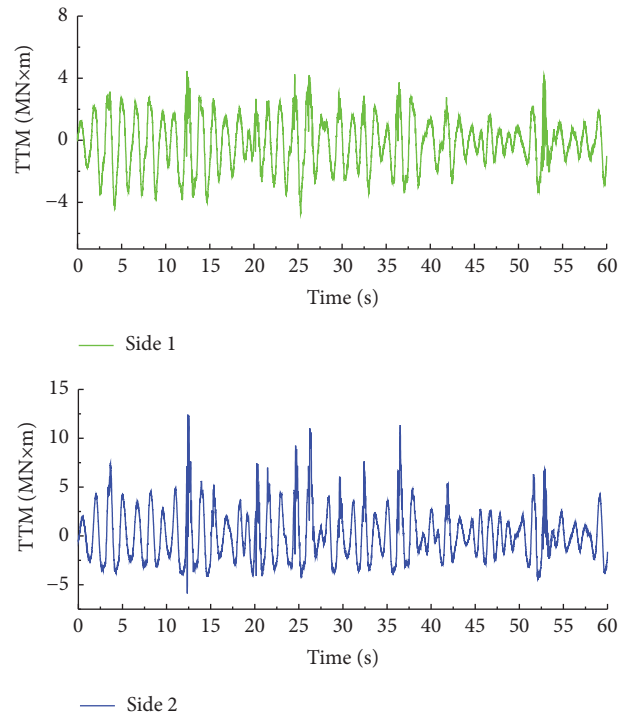


Figure 35: TTM time histories in beam sea.

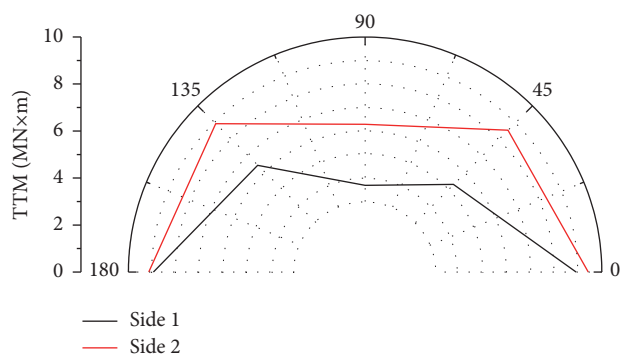


Figure 36: Transverse torsional moment in different azimuths.

of hydroelasticity on transverse bending deformation is not severe in oblique waves.

*(2) Transverse Torsional Moment.* The transverse torsion deformation is also monitored by the transverse backbone system. The time history data of transverse torsional moment is observed and shown in Figure 35. The peak of transverse torsional moment is still at the same time like splitting moment. And the minimum of the transverse torsional moment in different azimuths is found in beam sea by observing Figure 36. The TTM of cross-desk at side 2 is approximately 1.5 times as much as the one at side 1 in oblique waves. And the TTM in oblique waves grows gently when ship suffers higher waves.

The power spectral density functions of TTM are shown in Figure 37. The high frequency peak (8.67 Hz) appears at side 2 but cannot be found at side 1. Therefore, it is concluded that it is highly possible for transverse torsional moment at the wave forward surface to cause elastic vibration.

*3.3. Wave Impact of Trimaran under Irregular Waves.* The impact of waves always causes high frequency vibration. And the high frequency vibration accelerates the fatigue failure of trimaran's structure. By arranging the pressure gauges on the shell of trimaran model, the rule of wave impact is studied.

The pressure sensors 1–10 are arranged at three cross-sections to observe the rule of pressure at the bow segment. The first cross-section includes the pressure sensors 1–3, whose locations are above the waterline. The number 1 pressure sensor, whose location is lowest in the three sensors, suffers more types of wave impact in the three pressure sensors. And the three pressure sensors reached the maximum value at 63.48 s, as seen in Figure 38. And Figure 39 shows the moment of trimaran model bow slamming. The bow of trimaran model rushed rapidly into the water and caused bow slamming, as shown in Figure 39(a). Then the model's bow emerged from water to finish the slamming phenomenon in Figure 39(b). The whole slamming process lasted 0.8 s approximately.

The vertical bending moment in the period of bow slamming is extracted and studied in Figure 40. The VBM also reaches the peak around the slamming moment, because the model encounters a high wave, which is also the reason of bow slamming. The Fourier filter is used to separate the wave load and the slamming load. The slamming load has great fluctuation at the slamming moment and then attenuates rapidly.

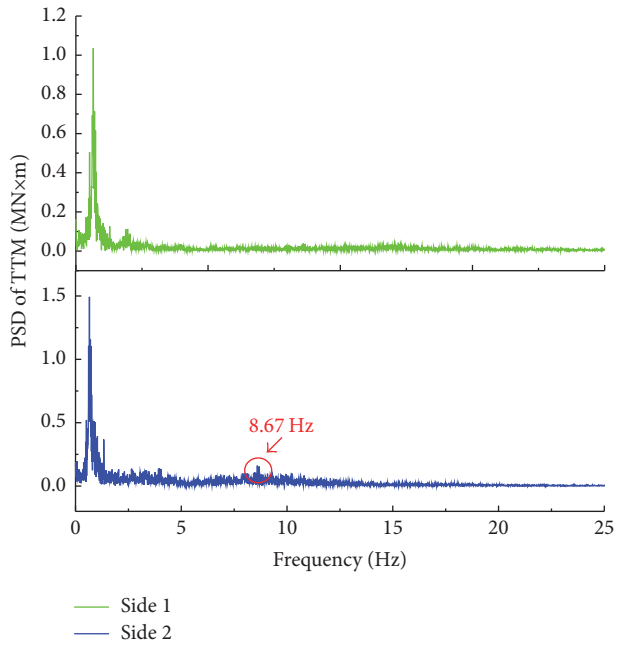


Figure 37: Power spectral density functions of TTM.

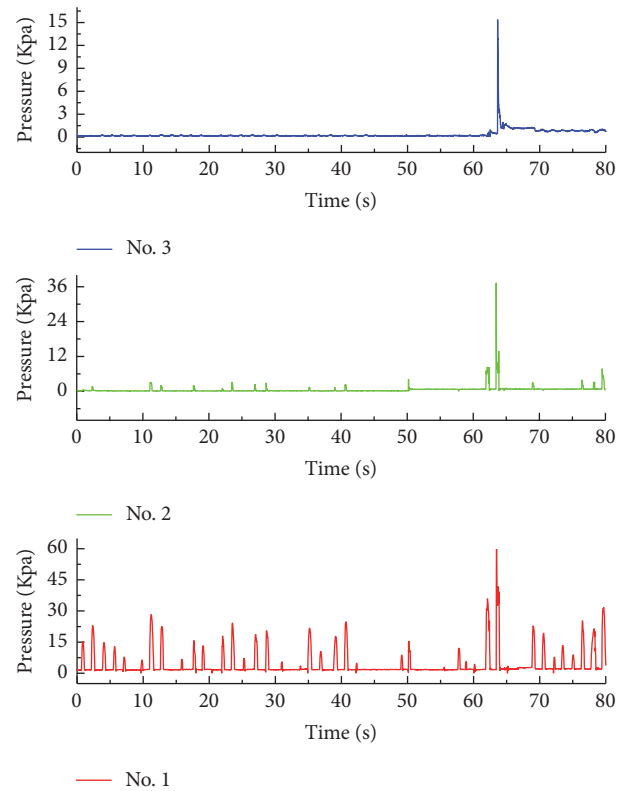


Figure 38: Time histories of pressure in bow sea.

In Figure 40(a), the measured VBM at P1 reach the maximum peak (6.657 MN × m) at 63.49 s. And the value of wave load is 4.239 MN × m at the same moment, which is not the maximum peak of wave load during this period. The slamming load causes the deviation of load peak time between total load and wave load. In addition, the amplitude of total load increases 36.32% by comparing the difference between the measured load and the wave load. This enhancement considers the comprehensive influence on amplitude and phase of both wave load and slamming load at slamming moment. The enhancement ratio at bow is variable and even can reach 88.01% at some moment. Therefore, the slamming load is an important component for total load at bow. The influence of slamming load amidships is also analyzed in Figure 40(b). The measured VBM at P4 reach the maximum peak at 63.93 s. The moment of maximum peak amidships is later than the moment at bow. And the enhancement ratio of this slamming moment at P4 is 15.61% by comparing the difference between the measured load and the wave load. Obviously, the proportion of the slamming load is decreased gradually compared with the proportion at bow. In fact, the wave load is the primary component for measured load amidships. And the slamming load is an indispensable component, which cannot be ignored.

The similar relationship is found between the slamming of cross-deck and the splitting moment on transverse structure. The whipping response in transverse structure also exists by the slamming on cross-deck. From Table 4, it can be found that there is a downward trend of pressure with the increase of the ship vertical height in the three oblique wave conditions. The rule is also fit for the number 4–6 pressure sensors in second cross-section. The three sensors (numbers 8–10) in the third cross-section are arranged near the waterline. Number 9 sensor at the waterline always suffers more

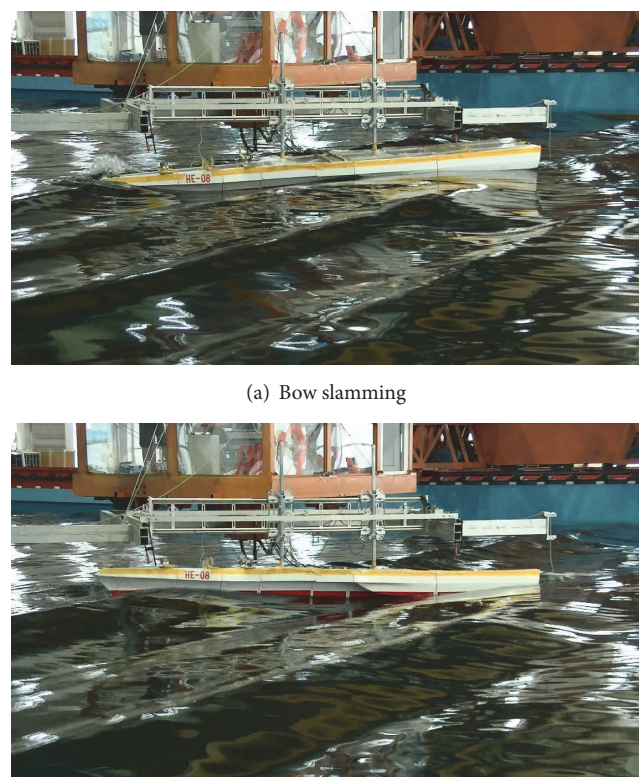

(a) Bow slamming

(b) Bow emerges from water after slamming

Figure 39: Bow slamming in bow sea.

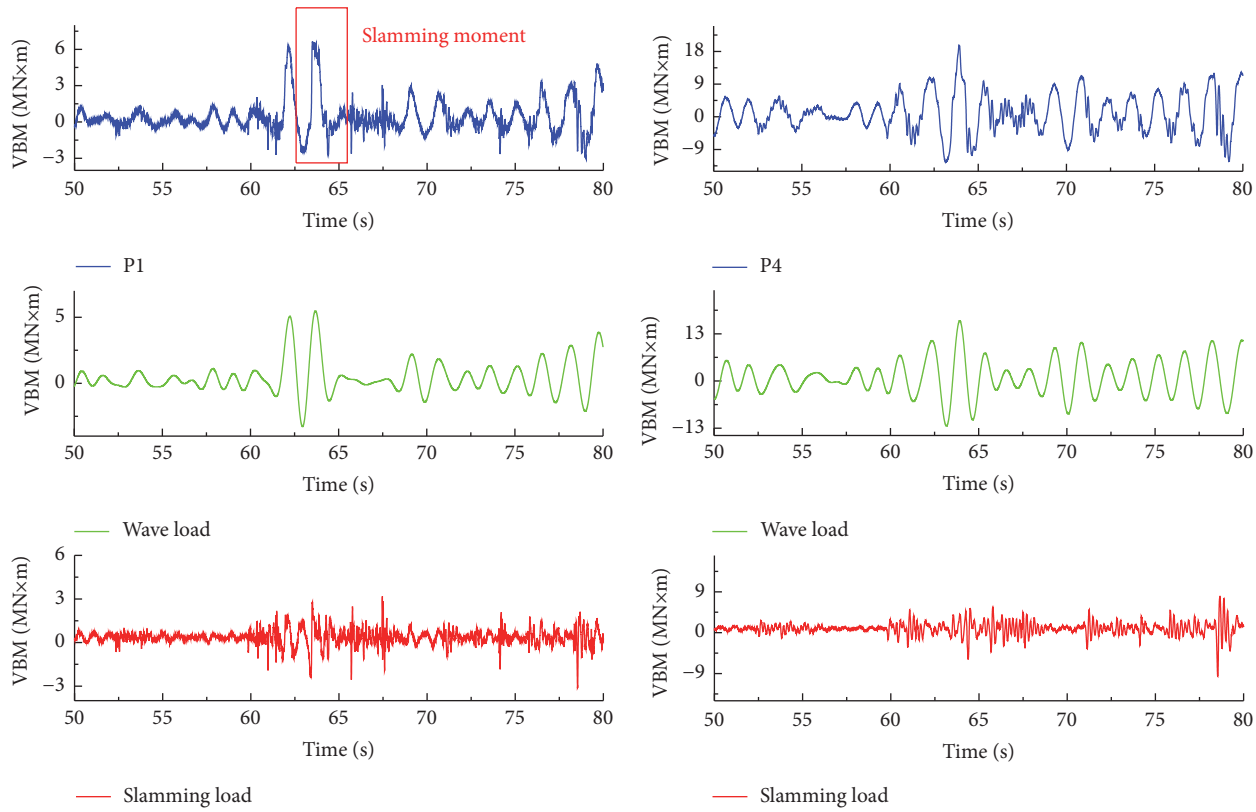


(a) VBM time histories at bow

(b) VBM time histories amidships

Figure 40: VBM time histories at slamming moment.

Table 4: Pressure in different azimuths.

| Number | Pressure (Kpa) | | |
|---|---|---|---|
| | Bow sea | Beam sea | Quartering sea |
| 1 | 59.86 | 24.37 | 29.60 |
| 2 | 37.33 | 20.85 | 25.64 |
| 3 | 15.38 | 0.00 | 0.00 |
| 4 | 36.93 | 28.03 | 27.65 |
| 5 | 30.54 | 21.45 | 22.10 |
| 6 | 26.41 | 15.32 | 20.28 |
| 7 | 34.13 | 20.73 | 26.93 |
| 8 | 29.03 | 19.45 | 25.65 |
| 9 | 30.18 | 25.24 | 26.17 |
| 10 | 25.67 | 16.44 | 21.24 |
| 11 | 23.48 | 18.99 | 23.82 |
| 12 | 25.65 | 22.94 | 28.70 |
| 13 | 20.38 | 16.75 | 21.06 |
| 14 | 17.85 | 10.43 | 18.06 |
| 15 | 28.77 | 25.43 | 31.34 |
| 16 | 36.39 | 30.74 | 38.74 |
| 17 | 23.14 | 19.83 | 24.56 |
| 18 | 18.81 | 10.02 | 19.48 |
| 19 | 20.79 | 14.88 | 20.99 |
| 20 | 18.32 | 17.34 | 23.22 |

severe wave impact by comparing the pressure of number 8 sensor and number 10 sensor at the same cross-section. The phenomenon is also found in other pressure sensors at waterline, such as number 12 pressure sensor and number 16 pressure sensor. Number 7 pressure sensor monitors the bottom slamming of trimaran's bow. Its pressure in beam sea is insensitive compared with the pressure in other azimuths. The low response of pitch in beam sea can explain the phenomenon. The bow slamming is weaker when the sensors location is far from bow at the first segment by analyzing the pressure in number 1 pressure sensor, number 5 pressure sensor, and number 10 pressure sensor, which are at the same depth. But for the slamming distribution along the ship length, the pressure will rebound at stern by observing the pressure of number 16 pressure sensor. The phenomenon can be explained where the slamming of side hull influences the wave impact of main hull at stern and increases the pressure in cross-deck channel. The slamming at cross-desk is recorded by number 18 pressure sensor. This slamming is more sensitive in the quartering sea than the other azimuths. The difference of pressure of number 19 pressure sensor and number 20 pressure sensor is the result of multiple influences. The oblique wave condition often raises the pressure of side hull at outside surface, especially in the beam sea. So the pressure of the side hull at outside surface is higher than the one at inside surface in beam sea and quartering sea. But the mutual interference between the main hull and side hull

also makes the wave impact more severe at inside surface of side hull. It can be explained that the pressure of number 19 pressure sensor is higher than the pressure of number 20 pressure sensor in bow sea.

## 4. Conclusions

In this paper, the trimaran's response of motion and wave-induced vibration in irregular oblique waves was studied by experiment. A scaled segmented trimaran model that matched the vibration characteristics of prototype was designed and tested in tank with different azimuths and wave heights. The experimental results of motion, load, and wave impact are analyzed, respectively. And the conclusions are made as follows:

(1) The motion of trimaran with side hull at stern has its own characteristics in oblique waves. The motion of heave and roll in beam sea is more sensitive than the response of other azimuths. And the following sea condition is the most dangerous case for the trimaran motion of pitch. In oblique waves, the bow acceleration is motivated most intensely in quartering sea and beam sea and replaced by stern acceleration in bow sea.

(2) The different kinds of vibration deformation should be considered separately in oblique waves. The position amidships always suffers vertical bending deformation most severely, and the maximum torsional deformation often happens at stern. But the longitudinal distribution of horizontal bending deformation is not stable and changes with different azimuths. In oblique waves, the bow sea condition often causes more severe vertical and horizontal bending vibration than the response in other oblique wave conditions. And the consistent fluctuation of vertical bending vibration between the main hull and side hull exists. The vertical bending vibration of side hull makes an important contribution to total vertical bending vibration at stern and cannot be ignored. Through spectral analysis, the hydroelastic vibrations are found in VBM and HBM. The springing effect should be paid more attention in the structure strength assessment of vertical and horizontal bending deformation.

(3) The characteristics of transverse deformation in oblique waves should be concerned. The splitting moment reaches a maximum peak in beam sea and tends to gentle in quartering sea with increase of wave height. And the transverse torsional moment in beam sea gets minimum with different azimuths. The cross-bridge structure at wave forward side always suffers more severe transverse deformation and should be strengthened in structural design.

(4) The drastic slamming and the severe high frequency impact load will appear, when ship encounters high waves. The enormous instantaneous loads caused by whipping increase the total load greatly at the slamming moment and should be taken seriously for the structural assessment. In addition, the local structure of trimaran's shell near the waterline and at stern should be strengthened to resist more violent wave impact.

In the present research, all the experiment is based on low speed to ensure relative position invariant. The irregular wave response of vibration and slamming in different high speed will be studied in further research. More factors that cause load nonlinearity will be recorded to make the experiment results more credible.

## Competing Interests

The authors declare that there is no conflict of interests regarding the publication of this paper.

## Acknowledgments

This research was supported by the National Natural Science Foundations of China (nos. 51209054 and 51079034). The authors express their gratitude to these foundations.

## References

[1] X. P. Lu, Y. Li, and Z. S. Dong, "A reseach summary on high speed trimaran," *Journal of Naval University of Engineering*, vol. 17, no. 2, pp. 43–44, 2005.

[2] J. Hampshire, S. Erskine, N. Halliday, and M. Arason, "Trimaran structural design and assessment," *Design & Operation of Trimaran Ships*, pp. 55–61, 2004.

[3] C. Kennell, "Model test result for a 55 knot high speed sealift trimaran," in *Design & Operation of Trimaran Ships*, pp. 195–203, 2004.

[4] X. L. Wang, J. J. Hu, Y. C. Geng, and C. Xu, "Experimental investigation of wave induced loads of a trimaran," in *Proceedings of the Conference of China Steel Structure Association on Marine Steel Structure Branch*, pp. 47–54, Luoyang, China, 2010.

[5] J. J. Hu, X. L. Wang, F. Zhang, and C. Xu, "Wave-induced loads forecast and design loads determine based on the model test of a trimaran," in *Proceedings of the Conference of China Steel Structure Association on Marine Steel Structure Branch*, pp. 61–69, Luoyang, China, 2010.

[6] X. L. Wang, J. J. Hu, X. C. Gu, Y. C. Geng, and C. Xu, "Comparative studies of the transverse structure design wave loads for a trimaran by model tests and rule calculations," *Journal of Ship Mechanics*, vol. 15, no. 3, pp. 269–274, 2011.

[7] S. Peng, W. Wu, H. Sun, J. Pan, and Z. Xia, "Experimental study and numerical simulation on slamming of trimaran," in *Proceedings of the 21st International Offshore and Polar Engineering Conference (ISOPE '11)*, pp. 881–886, Maui, Hawaii, USA, June 2011.

[8] H. Yu, Z.-J. Li, J.-J. Hu, and H.-L. Si, "Slamming load forecasts and analyses of a trimaran model test," *Journal of Ship Mechanics*, vol. 18, no. 6, pp. 623–634, 2014.

[9] Z. Y. Chen and H. L. Ren, "Wave load experimental investigation of a segmented model of a very large ship based on variable cross-section beams," *Journal of Harbin Engineering University*, vol. 33, no. 3, pp. 263–268, 2012.

[10] J. L. Jiao, H. L. Ren, and A. A. Christiaan, "Experimental and numerical analysis of hull girder vibrations and bow impact of

a large ship sailing in waves," *Shock and Vibration*, vol. 2015, Article ID 706163, 10 pages, 2015.

[11] H. L. Ren and Z. Y. Chen, "Effect of self-propulsion and towing test on ship load response," *Journal of Huazhong University of Science and Technology*, vol. 40, no. 11, pp. 85–88, 2012.

[12] W. P. Zhang, Z. Zhong, and S. L. Ni, "Model testing of seakeeping performance of trinaran," *Journal of Hydrodynamics A*, vol. 22, no. 5, pp. 619–624, 2007.

[13] K. A. Vakilabadi, M. R. Khedmati, and M. S. Seif, "Experimental study on heave and pitch motion characteristics of a wave-piercing trimaran," *Transactions of Famena*, vol. 38, no. 3, pp. 13–26, 2014.

[14] Z.-Y. Chen, H.-L. Ren, and F.-S. Sun, "Model experiment of time distribution of flare slamming," *Journal of Shanghai Jiaotong University*, vol. 47, no. 6, pp. 904–908, 2013.

[15] Z.-Y. Chen, H.-L. Ren, H. Li, and K.-H. Zhang, "Experimental and numerical analysis of bow slamming and whipping in different sea states," *Journal of Ship Mechanics*, vol. 16, no. 3, pp. 246–253, 2012.

[16] Y. X. Yu, *Random Wave and Its Applications to Engineering*, Dalian University of Technology Press, Dalian, China, 1992.

[17] Y. S. Dai, J. W. Shen, and J. Z. Song, *Ship Wave Loads*, National Defend Industry Press, Beijing, China, 2007.